Eur. Phys. J. Spec. Top. (2026) 235:2637–2651
https://doi.org/10.1140/epjs/s11734-025-02099-5

THE EUROPEAN PHYSICAL JOURNAL SPECIAL TOPICS

Regular Article

An algebraic generalisation of the Krankheit-operator modelling neurological disorders

Maria Mannone[1,2,3,a] and Thomas Mach[4]

[1] ICAR, National Research Council of Italy (CNR), Palermo, Italy
[2] Institute of Physics and Astronomy, University of Potsdam, Potsdam, Germany
[3] Potsdam Institute for Climate Impact Research (PIK), Member of the Leibniz Association, Potsdam, Germany
[4] Institute of Mathematics, University of Potsdam, Potsdam, Germany

Received 16 September 2025 / Accepted 8 December 2025 / Published online 4 February 2026

Abstract Several neurological disorders can be described as alterations of the brain connectome, both anatomic and functional. To model diseases and compare them, it has been proposed the *Krankheit*-operator (K-operator), which acts on the weights of the connectome, reproducing the effects of specific disorders. In this article, with algebraic tools, we attempt to provide a more general definition of the operator, that encompasses the previous different definitions provided. We consider a general setting where the linear operator is an endomorphism on the vector space of $n \times n$ matrices. We show that the left and right matrix multiplication and a Hadamard multiplications can all be described as a special structured operator.

1 Introduction

The existence of different perspectives on a phenomenon can often hint towards the existence of a more general view. It is the case of studies on the brain, including mathematical and physics-inspired modelling of its nested structure, with neurons, neuronal agglomerates, and lobes. And it is thus the case of a graph-based description of the key neuronal macro-agglomerates and the links between them, constituting the so-called brain connectome [21]. The alteration of anatomic and especially functional brain networks [1] can be related with the onset and development of neuropsychiatric and neurodegenerative diseases. This is one of the aims of computational psychiatry [10], and of the analysis of alterations of graph neural networks for connectome-based brain disorders [5].

Thus, the action of a disease may change the brain in all facets. We are particularly interested in the changes to the brain connectome.

To model the action of disease on the brain connectome, a new approach object has been recently proposed. In analogy with the definitions of operators in physics, acting on observables corresponding to physical quantities, and acting on them producing changes, it has been defined a mathematical object acting on the human brain to produce changes typical of neurological disorders. The K-operator—or more precisely the restriction of the K-operator to the brain connectome—is, in fact, defined as a mathematical object, in the form of an operator, that acts on a healthy brain altering it, reproducing the effects of a disease. In particular, we can consider the weights of the connections between the brain areas [14]. In this case, the operator maps from the set of $n \times n$ matrices to the set of $n \times n$ matrices. Since domain and co-domain are equal, this homomorphism is called *endomorphism*. If it is bijective, it is an *automorphism*. Alternatively, we consider a modelling of the K-operator as automorphism on the set of correlation matrices.

The disease alters the connectivity of the brain and thus the correlation matrix describing the connections. Whilst each pathological brain evolution is different, and thus, each instance of the K-operator is different, the evolution of brains affected by the same disorder presents similarities. Thus, we will have a class of operators with key similarities (as having elements targeting specific brain areas in a similar way over time), as signature elements characterising a specific disease. Thus, similar disorders will share similarities at the level of K [15].

Specific instances of the K-operator have been computed from data of selected patients affected by Alzheimer–Perusini's disease [16], Parkinson's disease [13], schizophrenia [13], and, with some adaptation, epilepsy [18]. It

[a] e-mail: maria.mannone@icar.cnr.it (corresponding author)

has also been proposed a space of brain states, thinking of the phase space in physics, whose first computational implementation uses the multi-dimensional scaling [17]. An analysis of patterns of eigenvalues from different definitions of the K-operator, and the recurrence plot-analysis of time-series from brain regions selected upon visual inspection of K, has been proposed in [6].

However, in the aforementioned recent literature, different versions of the K-operator have been used, and the visualisations obtained from them present empiric correspondences. Each definition highlights some elements, but hinders others, or poses some difficulty of interpretation. In this article, we aim to first propose a formal relationship between the definitions, and then to lay the foundations of a more general definition of the operator, that encompasses the previous ones.

This position paper aims thus to face some of the open issues of the newly proposed operator, and it is organised as follows. In Sect. 2, we list and illustrate the current definitions of the K-operator. An example of their implementation with real data is provided in Sect. 3. A further example with synthetic data, and a first formalisation of a relationship between them, is given in Sect. 4. The core of the article is the more comprehensive theoretical approach, proposed in Sect. 5. A short Discussion (Sect. 6) on the next line of research development ends the article.

2 Current definitions of the K-operator

The K-operator is defined as a matrix operator that acts on a healthy brain, giving as output a diseased one [14]:

$$K := K|_{\text{connectome}} : \mathbb{R}^{n\times n} \to \mathbb{R}^{n\times n} : \mathcal{G} \to \mathcal{G}^k, \tag{1}$$

we write

$$K\mathcal{G} = \mathcal{G}^k, \tag{2}$$

where $\mathcal{G}$ is a matrix representing a healthy brain, and $\mathcal{G}^k$ a diseased one, with k as a label for *Krankheit*, *disease*. From now on, we only consider the restriction of the disease operator on the connectome and thus omit the restriction when using K. Considering time progression of the disease, we can write:

$$K(t)\mathcal{G}^k(t) = \mathcal{G}^k(t+1). \tag{3}$$

This notation can be understood in two different ways. On the one hand, we can consider $K(t)$ to be an operator acting on $\mathcal{G}^k(t)$, that is $K(t)\colon \mathbb{R}^{n\times n} \to \mathbb{R}^{n\times n}$. On the other hand, we can consider $K(t)$ to be a matrix $K(t) \in \mathbb{R}^{n\times n}$ and $K(t)\mathcal{G}^k(t)$ to be a matrix–matrix product. Below, both options are discussed. The matrices $\mathcal{G}^k(t)$ describing the (state of the) brain are derived from experimental data. For instance, focussing on functional connectivity, the brain matrices will be the connectivity matrices containing, as elements, the weights of the (directed or undirected) links between brain nodes. Other choices for the brain matrices $\mathcal{G}^k(t)$, which can also be related to the results of cognitive tests, are possible but beyond the scope of this paper.

Experimentally, as discussed in detail in [13], the starting point is the folder of image files of resting-state fMRI, in form of DICOM files (DICOM stands for Digital Imaging and Communications in Medicine). They contain information on the blood movement over time, corresponding to the activation of specific brain areas. They are then converted into NIfTI files (where the acronym stands for Neuroimaging Informatics Technology Initiative), and, through the choice of a specific medical atlas, that is, particular grouping of pixels, time series in each brain regions are extracted. Through the computation of the Pearson correlation between pairs of time series, we can finally obtain a connectivity matrix, to be used here as an instance of the $\mathcal{G}$ or $\mathcal{G}^k$ matrix. Thus, we can adopt correlation matrices as the $\mathcal{G}$-matrices, containing the averaged information on the correlation between the activity of pairs of brain areas, corresponding to a time point. In fact, we distinguish between the time flowing for time series, and corresponding to the time within the window of observation of the brain inside the magnetic resonance machine, and the time of the year when the measurement is performed. Two fMRIs performed at distance of 6 months, for instance, will lead to $\mathcal{G}$ at two different time points.

Once the matrices of healthy and diseased brains are known, a shape of the operator can be approximated as a numeric matrix. The first approach involves the matrix inversion and the matrix product:

$$\mathcal{G}^k = K_\ell\mathcal{G} \implies K_\ell = \mathcal{G}^k@\mathcal{G}^{-1}, \tag{4}$$

where here @ indicates the usual matrix product. We use an index to distinguish the matrix K_ℓ from similar matrices of size $n \times n$ representing the K-operator. However, the analysis of K_ℓ is not easy, as the rows and columns of $\mathcal{G}$-matrices, containing labels of the brain areas, are mixed due to the matrix product. One way to interpret K_ℓ is to regard it as a remixing of the outgoing connections from each domain. This, however, has

limited explanatory power, since, at the same time, the incoming connections would have to be remixed to preserve symmetry. We attempt to overcome this in the next section. In addition, it has been experimentally observed that the rows of the K-operator computed with (4) correspond to the clusters of higher values that can be obtained whilst using the Hadamard product within the same expression; see (5) [13,16]:

$$K_m = \mathcal{G}^k \odot \mathcal{G}^{-1}, \tag{5}$$

where we use the symbol $\odot$ to indicate the Hadamard or entry-wise product. As above, K_m is an $n \times n$ matrix representing the K-operator.

Let $K_{mixed} = \mathcal{G}^k \odot \mathcal{G}^{-1}$ and $K_{mix,eq} = \mathcal{G} \odot \mathcal{G}^{-1} \neq \mathbb{I}$. If $\mathcal{G} = \mathcal{G}^k$, then $K_{mixed} = K_{mix,eq}$. However, in general, $\mathcal{G} \neq \mathcal{G}^k$, and we can write: $K_{mixed} - K_{mix,eq} = (\mathcal{G}^k - \mathcal{G}) \odot \mathcal{G}^{-1}$, which can help isolate the effect of $\mathcal{G} \to \mathcal{G}^k$.

The results obtained with (5) are easy to interpret, given the preserved correspondence of labels of rows and columns with the considered regions of the brain, but the formula itself is not mathematically precise, given the coexistence of an inverse matrix and of the Hadamard product. A third application concerns the use of a "purely Hadamard" product, where each element of K is obtained as the ratio of the brain matrices [18]:

$$\mathcal{G}^k = K_\odot \odot \mathcal{G} \implies K_\odot = \mathcal{G}^k \oslash \mathcal{G} \iff K_\odot|_{ij} = \frac{\mathcal{G}^k_{ij}}{\mathcal{G}_{ij}}, \tag{6}$$

where $\oslash$ indicates the entry-wise division and $K_\odot|_{ij}$ is the entry of the matrix $K_\odot$ in row i and column j. The comparison between the three cases shows vertical correspondences. These first results point towards the exigence for a more comprehensive, general definition of the operator, to be mathematically precise yet understandable from a point of view of the neurosciences.

3 An example

To give a further idea of the hidden analogies between the three definitions of K, and to emphasise the neurological relevance of the problem of finding a unitary description of the operator, we propose here an example of application. We consider as $\mathcal{G}$ the connectivity matrix obtained from the functional magnetic resonance, resting state (fMRI-rs), of a healthy person, and as $\mathcal{G}^k$, the corresponding connectivity matrix from a Parkinsonian patient (PD). The healthy control is subject subMJF044, female, 66 years old, and the PD patient is subject subMJF020, a Parkinson's disease (PD), female, 69 years old, without cognitive issues, that is, normal control (NC), and thus classified in the dataset as a PD-NC. The original data are taken from the platform OpenNeuro [12].[1] As the choice of atlas, we consider the Multi-subject Dictionary learning (MSDL) atlas [23], constituted by 39 regions of interest (ROIs) in which the brain can be divided into. See Table 1 for their list, Algorithm 1 for the method, and Fig. 1 for the matrices $\mathcal{G}$ and $\mathcal{G}^k$, and the three computations of K.

Algorithm 1 Computing specific forms of the K-operator [13,17]

```
choose brain atlas
for each fMRI set of measurements do
    compute NIfTI file
    use the atlas as a mask, extract time series for each ROI
    compute correlation between pairs of ROIs
    average over time
    print connectivity matrix
    label it 𝒢 or 𝒢^k according to the dataset "healthy/diseased" labelling
end for
for pairs of 𝒢, 𝒢^k or longitudinal 𝒢^k(t), 𝒢^k(t+1) do
    compute the K-operator
    analyse its entries
end for
```

In the literature on the K-operator [13,16], empiric thresholds had been used to highlight the entries of the operator presenting the higher changes in absolute value. However, here, we do not choose any threshold, being

[1] https://openneuro.org/datasets/ds005892/versions/1.0.0.

Table 1 ROIs for the MSDL atlas [23]

ROI	tag	complete name
0	L Aud	Left Auditory Cortex
1	R Aud	Right Auditory Cortex
2	Striate	Striate Cortex
3	L DMN	Left Default Model Network
4	Med DMN	Medial Default Model Network
5	Front DMN	Frontal Default Model Network
6	R DMN	Right Default Model Network
7	Occ post	Occipital Posterior
8	Motor	Motor Cortex
9	R DLPFC	Right Dorsolateral Prefrontal Cortex
10	R Front pol	Right Frontal Pole
11	R Par	Right Parietal
12	R Post Temp	Right Posterior Temporal
13	Basal	Basal Ganglia
14	L Par	Left Parietal
15	L DLPFC	Left Dorsolateral Prefrontal Cortex
16	L Front pol	Left Frontal Pole
17	L IPS	Left Intra-parietal Sulcus
18	R IPS	Right Intra-parietal Sulcus
19	L LOC	Left Lateral Occipital Cortex
20	Vis	Visual Cortex (lingual gyrus)
21	R LOC	Right Lateral Occipital Cortex
22	D ACC	Dorsal Anterior Cingulate Cortex
23	V ACC	Ventral Anterior Cingulate Cortex
24	R A Ins	Right Anterior Insula
25	L STS	Left Superior Temporal Sulcus
26	R STS	Right Superior Temporal Sulcus
27	L TPJ	Left Temporo-parietal Junction
28	Broca	Broca's area
29	Sup Front S	Superior Frontal Sulcus
30	R TPJ	Right Temporo-parietal Junction
31	R Pars Op	Right Pars Opercularis
32	Cereb	Cerebellum
33	Dors PCC	Dorsal Posterior Cingulate Cortex
34	L Ins	Left Insula
35	Cing	Cingulate Cortex
36	R Ins	Right Insula
37	L Ant IPS	Left Anterior Intra-parietal Sulcus
38	R Ant IPS	Right Anterior Intra-parietal Sulcus

more interested in the "original" configuration of the operators. We only changed the scaling, to highlight the pattern distribution. Some correspondences between isolated elements encapsulating the bigger changes of entries of the initial matrices are still visible, as single points for $K_{\odot}$, and blocks for K_l and K_{mix}.

From the observation of Fig. 1, we notice that some of the places where K_l presents high values correspond vertically with some high-changing entries of K_{mix} and $K_{mix} - \mathcal{G} \odot \mathcal{G}^{-1}$, with smaller values overall, though. Comparing K_l with $K_{\odot}$, we notice that the structure has been somehow pruned, isolating the regions where the effects of disease are more evident. The larger entries of $K_{\odot}$ correspond to those core hubs where the effect of disease is more evident. And this is coherent with the formal definition, as this is the purely entry-wise operator. In particular, from the observation of $K_{\odot}$, we notice an alteration of connectivity between the posterior cingulate cortex (33) and the medial default mode network (4), and concerning occipital cortex, in particular the visual cortex (20), the right parietal (11), and the intra-parietal sulcus (37, 38). The literature confirms the presence of alterations of the resting-state functional connectivity in posterior cingulate cortex for PD patients [27], related to mild dementia. The considered patient was a normal-cognition PD, but a mild alteration of these pathways could be early signalled, as a biomarker for its early signs of cognitive issues. $K_{mix} - \mathcal{G} \odot \mathcal{G}^{-1}$ also signals a presence of alteration concerning the connectivity of the precentral gyrus, a key motor area, affected by PD [25]. The common information emerging from K_l, $K_{mix} - \mathcal{G} \odot \mathcal{G}^{-1}$, and $K_{\odot}$ concerns overall the default mode network, the visual network, the fronto-parietal area, and the salience network, with right anterior insula and dorsal anterior cingulate

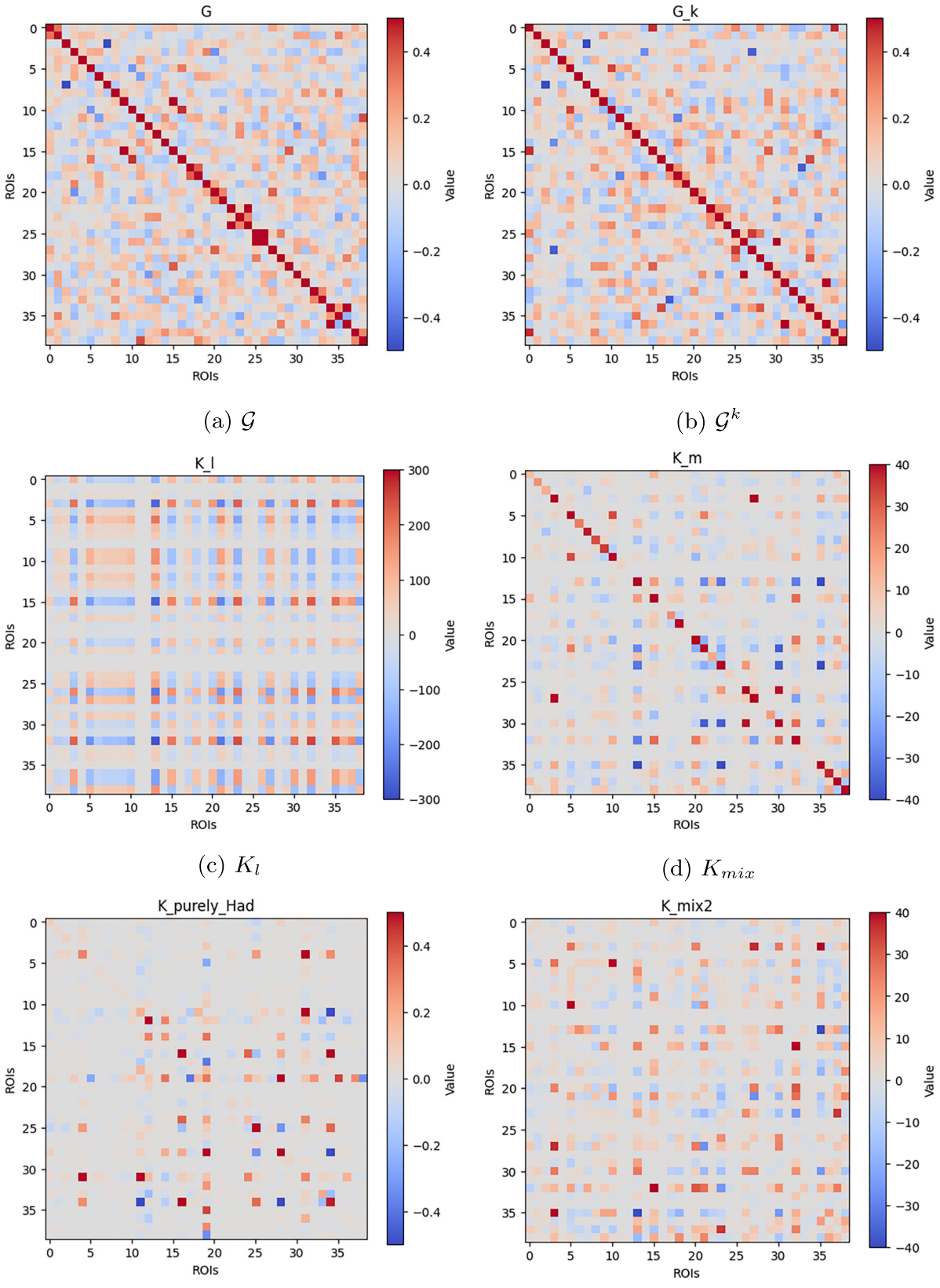

(a) $\mathcal{G}$ (b) $\mathcal{G}^k$

(c) K_l (d) K_{mix}

(e) $K_{\odot}$ (f) $K_{mix} - \mathcal{G} \odot \mathcal{G}^{-1}$

Fig. 1 Initial matrices from real data: healthy control (**a**) and a PD patient without cognitive issues (**b**), and the versions of the K-operator derived from them (**c**–**e**). We also show the difference between K_{mix} and $\mathcal{G} \odot \mathcal{G}^{-1}$ (**f**). The meaning of each region of interest (ROI) is presented in Table 1

cortex, all relevant for PD. In particular, damage concerning the insula pathways, and especially its right side, can be caused by dopaminergic alterations occurring in PD [22], given the strong connections with the globus pallidus. The functioning of the latter is harmed by the reduction of dopamine from the substantia nigra, a key feature of Parkinson's disease.

In addition, to further investigate the key features of each product, at the basis of the definitions of the K-operator, we define here three new operators. We will assess their action on a grouping of the brain areas of MSDL atlas, to assess the change in each grouping indicated by each kind of product. In particular, let $R, M, L \in \mathbb{R}^{n\times n}$ be the three operators whose entries are defined as follows:

$$R_{ij} = \Delta_{ij}/\mathcal{G}_{ij},\ M_{ij} = \Delta_{ij}\mathcal{G}_{ij}^{-1},\ L_{ij} = \sum_p \Delta_{ip}\mathcal{G}_{pj}^{-1}, \tag{7}$$

where $\Delta = \mathcal{G}^k - \mathcal{G}$. Also, let $\mathcal{S} = \{s_1, s_2, \ldots, s_z\}$ be the set of $z = 11$ groupings of the $n = 39$ ROIs of the MSDL atlas. Each grouping s constitutes a specific brain system. Let V_s be the set of ROIs belonging to the sth system. For each ROI, we can define a mean value of R, M, L. The system-level average for s is given by

$$R_{\text{mean}}(s) = \frac{1}{|V_s|}\sum_{i\in V_s} R_i,\ M_{\text{mean}}(s) = \frac{1}{|V_s|}\sum_{i\in V_s} M_i,\ L_{\text{mean}}(s) = \frac{1}{|V_s|}\sum_{i\in V_s} L_i, \tag{8}$$

where V_s is the set of ROIs (the vertices of the connectome) in each system s, $|V_s|$ is its cardinality, which corresponds to the number of ROIs: $n = 39$. Conceptually, $R_{\text{mean}}(s)$ quantifies the average *relative change* of connectivity for all ROIs in system s; $M_{\text{mean}}(s)$ quantifies the average *precision-weighted change*, and finally, $L_{\text{mean}}(s)$ quantifies the average *propagated change*. With this information, using the code schematised in Algorithm 2, we obtain the histogram presented in Fig. 2.

Algorithm 2 Assessing the variations corresponding to the three products

```
for each 𝒢, 𝒢^k do
    compute Δ = 𝒢^k − 𝒢
    compute R, M, L as in Eq. (7)
    for each ROI i do
        compute its average change (row mean in R,M,L)
        group ROIs by system membership s
        take the mean of ROI values within each system
        show barplots.
    end for
end for
```

We notice, up to a difference of order of magnitude for each product, a correspondence of some of the brain groups that are more affected by the considered disease. In particular, the mixed product and the purely-entry-wise one are more effective to retrieve damage in the cerebellum. All the three kinds of product indicate a high-level damage in the subcortical area. Subcortical regions, such as thalamus, are also impacted by the disease. A previous study with the K-operator, based on more detailed atlases, pointed out towards alterations in connectivity of the pulvinar, one of the thalamic nuclei, as well as ventral anterior, ventral lateral left and right [13]. All this information points out to the need of exploring a more general definition of the K-operator, whose already existing definitions are specific instances, catching each one a specific aspect. Damage on visual area, that include occipital cortex, is associated with hallucinations, but this is not occurring in early stages of the disease, as for the considered patients. An alteration of occipital pathways at this stage could signal the onset of visuospatial difficulties. All the three kinds of operator indicate a very limited alteration to the visual area. Discrepancies between the first and the two other kinds of product concern the insula.

In general, complex disorders such as Parkinson's disease (PD) can be observed in light of both anatomic and functional alterations [19], also between cerebellar areas and substantia nigra, and with ventral tegmental areas in PD [20]. Further changes in a brain affected by PD concern the basal ganglia [3,7], the limbic system [2], the prefrontal cortex [11], and the cingulate cortex [24]. The comparative use of different definitions of the K-operator, already started in [13] for the first two products, confirmed findings of the medical literature, and could hopefully provide further information, especially concerning the prediction of disease progression, already performed in a study on AD [16]. In the next section, we will sketch a formal relationship between the three definitions, and then, a more general definition of the operator.

Table 2 Mapping of the ROIs of MSDL atlas with full region names, their corresponding ROI numbers (0–38), and a possible grouping of them

System	ROIs (MSDL numbers)
Auditory	Left Auditory Cortex (0), Right Auditory Cortex (1)
Visual	Striate Cortex (2), Left Lateral Occipital Cortex (19), Right Lateral Occipital Cortex (21), Occipital Posterior (7), Visual Cortex (20)
Default Mode Network (DMN)	Left DMN (3), Medial DMN (4), Front DMN (5), Right DMN (6), Dorsal Posterior Cingulate Cortex (33)
Motor	Motor Cortex (8)
Fronto-parietal / Control	Right Dorsolateral Prefrontal Cortex (9), Right Frontal Pole (10), Left Dorsolateral Prefrontal Cortex (15), Left Frontal Pole (16), Superior Frontal Sulcus (29)
Parietal	Right Parietal Cortex (11), Left Parietal Cortex (14), Left Intra-parietal Sulcus (17), Right Intra-parietal Sulcus (18), Left Anterior IPS (37), Right Anterior IPS (38)
Temporal	Right Posterior Temporal Cortex (12), Left Superior Temporal Sulcus (25), Right Superior Temporal Sulcus (26), Left Temporo-parietal Junction (27), Right Temporo-parietal Junction (30), Broca Area (28), Right Pars Opercularis (31)
Subcortical	Basal Ganglia (13)
Insula / Cingulate	Dorsal Anterior Cingulate Cortex (22), Ventral Anterior Cingulate Cortex (23), Right Anterior Insula (24), Left Insula (34), Cingulate Cortex (35), Right Insula (36)
Cerebellum	Cerebellum (32)

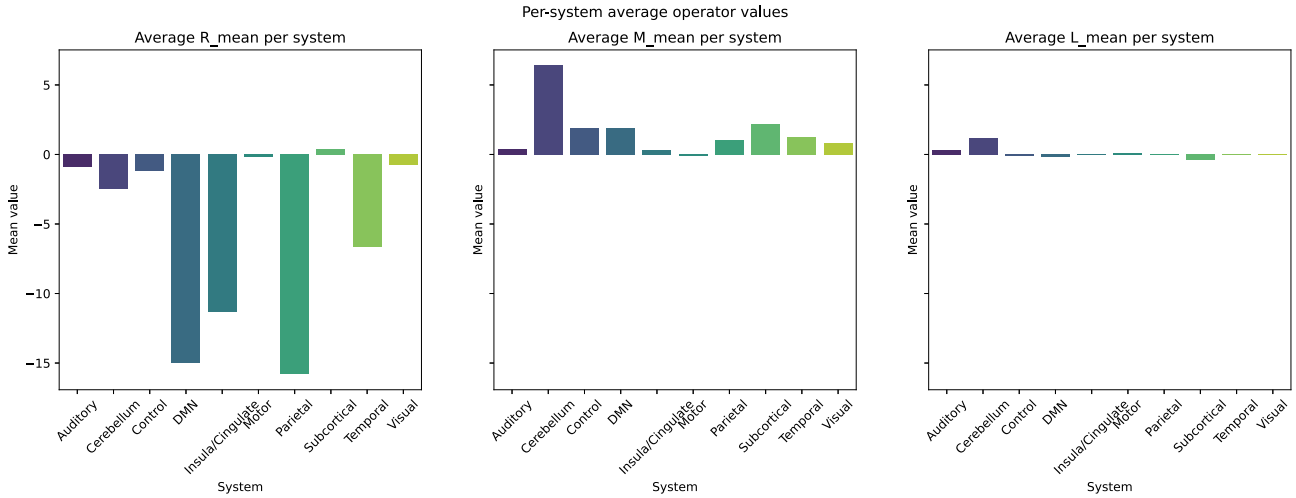

Fig. 2 Impact of the disease on groupings of ROIs (Table 2), according to different definitions of products, for the transition from a healthy person to a PD patient without cognitive issues. From left to right: purely entry-wise, mixed, and row-by-column

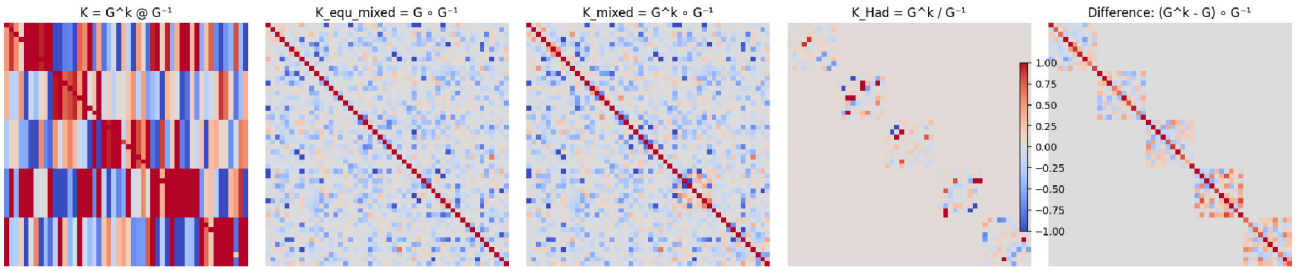

Fig. 3 Comparison between Ks as heatmaps and other tests on matrices. From left to right: K_l; K_m in the special case where $\mathcal{G}^k = \mathcal{G}$; K_m; $K_\odot$, and finally K_m from which the special case has been subtracted. The block correspondence between the first, the fourth, and the fifth heatmaps is evident

4 A relationship between the definitions of the K-operator

As an intermediate step before a generalisation of the theoretical approach, we first propose a heuristic comparison between Ks obtained from synthetic data, that is, $\mathcal{G}$ with random entries (null model) and a $\mathcal{G}^k$ with a block structure, as presented in Fig. 3.

We can approximate the transformation $\mathcal{G} \to \mathcal{G}^k$ as the result of a perturbation. Denoting with Δ the structural difference, we can write $\mathcal{G}^k = \mathcal{G} + \Delta$. The first product becomes:

$$K_\ell = \mathcal{G}^k \mathcal{G}^{-1} = (\mathcal{G} + \Delta)\mathcal{G}^{-1} = \mathbb{I} + (\Delta)(\mathcal{G}^{-1}), \tag{9}$$

where $\mathbb{I}$ is the identity matrix. The second product can be written as

$$K_m = \mathcal{G}^k \odot \mathcal{G}^{-1} = (\mathcal{G} + \Delta) \odot \mathcal{G}^{-1} = \mathcal{G} \odot \mathcal{G}^{-1} + \Delta \odot \mathcal{G}^{-1}. \tag{10}$$

Finally, the third product reads as

$$K_\odot = \mathcal{G}^k / \mathcal{G} = \mathcal{G}/\mathcal{G} + \Delta/\mathcal{G} = \mathbb{1}\!\!\mathbb{1} + \Delta/\mathcal{G}, \;\; K_\odot|_{ij} = \left(1 + \frac{\Delta_{ij}}{\mathcal{G}_{ij}}\right)_{ij}, \tag{11}$$

where $\mathbb{1}\!\!\mathbb{1}$ denotes the matrix having all elements equal to 1, whilst the identity matrix $\mathbb{I}$ has elements equal to 1 only on the diagonal. Rewriting (9) as $\Delta = (K_\ell - \mathbb{I})\mathcal{G}$ and substituting it into (10) and (11), we have respectively

$$\begin{aligned} K_m &= \Delta \odot \mathcal{G}^{-1} + \mathcal{G} \odot \mathcal{G}^{-1} = [(K_\ell - \mathbb{I})\mathcal{G}] \odot \mathcal{G}^{-1} + \mathcal{G} \odot \mathcal{G}^{-1} = \\ &= K_\ell \mathcal{G} \odot \mathcal{G}^{-1} - \mathcal{G} \odot \mathcal{G}^{-1} + \mathcal{G} \odot \mathcal{G}^{-1} = K_\ell \mathcal{G} \odot \mathcal{G}^{-1} \end{aligned} \tag{12}$$

and

$$\begin{aligned} K_\odot &= \Delta/\mathcal{G} + \mathbb{1}\!\!\mathbb{1} = [(K_\ell - \mathbb{I})\mathcal{G}]/\mathcal{G} + \mathbb{1}\!\!\mathbb{1} = \\ &= K_\ell \mathcal{G}/\mathcal{G} - \mathcal{G}/\mathcal{G} + \mathbb{1}\!\!\mathbb{1} = K_\ell \mathbb{1}\!\!\mathbb{1} - \mathbb{1}\!\!\mathbb{1} + \mathbb{1}\!\!\mathbb{1} = K_\ell \mathbb{1}\!\!\mathbb{1}. \end{aligned} \tag{13}$$

Thus, we get a first relationship between the Ks obtained with the different products

$$K_m = K_\ell \mathcal{G} \odot \mathcal{G}^{-1}, \;\; K_\odot = K_\ell \mathbb{1}\!\!\mathbb{1}. \tag{14}$$

5 A more comprehensive theoretical approach

As discussed above, we are describing the current state of a brain by the restriction to a correlation matrix $\mathcal{G}^k$ based on the interaction between different parts of the brain. This correlation matrix differs between individuals and changes over time based on ageing, environmental impacts, and diseases. We are particularly interested in the last part. However, ageing, environmental impacts, and differences between individuals are significant obstacles in revealing the K-operator. Correlation matrices from brain data are usually normalized between -1 and 1; we consider here a shift between 0 and 1.

A *correlation matrix* $\mathcal{G} \in \mathbb{R}^{n\times n}$ can be defined as a matrix of correlations between random variable (or time series) $X_1, \ldots, X_n$ with:

$$\mathcal{G}_{ij} = \mathrm{corr}(X_i, X_j) = \tfrac{1}{\sigma_i \sigma_j} \mathrm{cov}(X_i, X_j),$$

with σ_i the standard deviation of X_i, that is $\sigma_i = \sqrt{\mathrm{var}(X_i)} = \sqrt{\mathrm{cov}(X_i, X_i)}$.

Remark 1 A correlation matrix $\mathcal{G} \in \mathbb{R}^{n\times n}$ is

(i) symmetric,
(ii) positive semi-definite, and has
(iii) a unit diagonal.

Proof Part (i) follows from $\mathrm{corr}(X_i, X_j) = \mathrm{corr}(X_j, X_i)$. For part (ii), let $x \in \mathbb{R}^n$ and define a new random variable as linear combination $X = \sum_{i=1}^{n} x_i X_i$. The variance of X is non-negative and thus (ii) holds.
Finally, part (iii) follows from the fact that the $\mathrm{corr}(X_i, X_i) = 1$. □

Lemma 1 *Let $A \in \mathbb{R}^{n\times n}$ be a symmetric positive semi-definite matrix with unit diagonal, $A_{ii} = 1$ for all $i = 1, \ldots, n$. Then, all entries A_{ij} of A fulfil*

$$|A_{ij}| \leq 1.$$

Proof The proof is by contradiction. Let us assume there is an entry $|A_{ij}| > 1$. The submatrix

$$\begin{bmatrix} A_{ii} & A_{ij} \\ A_{ji} & A_{jj} \end{bmatrix} = \begin{bmatrix} 1 & A_{ij} \\ A_{ij} & 1 \end{bmatrix}$$

is symmetric and $\{(1 + A_{ij}), \begin{bmatrix} 1 \\ 1 \end{bmatrix}\}$ and $\{(1 - A_{ij}), \begin{bmatrix} 1 \\ -1 \end{bmatrix}\}$ are its eigenpairs. One of the two eigenvalues is less than zero. Thus, either for $x = e_i + e_j$ or for $x = e_i - e_j$, we have $x^T A x < 0$. This contradicts A positive semi-definite. □

Correlation matrices cannot be characterised by a unit diagonal and entries in $[-1, 1]$ without requiring positive semidefiniteness, since (see [9])

$$\begin{bmatrix} 1 & 1 & 0 \\ 1 & 1 & 1 \\ 0 & 1 & 1 \end{bmatrix}$$

is not a correlation matrix.

Let $A \in \mathbb{R}^{n\times n}$ be a symmetric positive definite matrix with unit diagonal. Then, there exists a Cholesky decomposition $A = LL^T$. Let $X_1, \ldots, X_n$ be n linearly independent random variables with mean zero and variance 1 each. Then, we can form random variables $\hat{X} = XL^T$, whereby the multiplication with the columns of L^T is to be understood as forming new linear combinations of the random variables X. The correlation matrix of the new random variables $\hat{X}_1, \ldots, \hat{X}_n$ is then the matrix A. Thus, all symmetric positive definite matrices with unit diagonal are correlation matrices.

Remark 2 The set of correlation matrices is closed and convex.

See, e.g., [9] for a proof.

We are now presenting a unified view on some of the different methods to define the K-operator. For this general view, we start with (2),

$$K\mathcal{G} = \mathcal{G}^k,$$

where $K : \mathbb{R}^{n\times n} \to \mathbb{R}^{n\times n}$ is a mapping from one $n \times n$ matrix to another one. A generalisation to the time-variant case $K(t)$ from (3) is possible. We assume that K is a linear operator. This allows us to write (2) as a matrix–vector product

$$\hat{K}\,\mathrm{vec}(\mathcal{G}) = \mathrm{vec}(\mathcal{G}^k), \tag{15}$$

where the vec operator is the vectorisation operator that concatenates the columns of a matrix into one long (column) vector. The matrix $\hat{K} \in \mathbb{R}^{n^2 \times n^2}$.

The Hadamard ansatz (6) fits the model (15) with the special structure that $\hat{K}$ is diagonal. The entries of $K_\odot$ from (5) can be recovered by

$$K_\odot|_{ij} = \hat{K}_\odot\Big|_{i+nj-n,i+nj-n}.$$

This argument works both ways. If we have a $\hat{K}$, we can ask: which is the closest $K_\odot$ to $\hat{K}$? This is the diagonal matrix defined by the diagonal entries of $\hat{K}$. This means given an arbitrary $\hat{K}$ we can partially interpret it by regarding its diagonal as $K_\odot$. Since the matrices $\mathcal{G}$ and $\mathcal{G}^k$ are symmetric, the operator $K_\odot$ has to be symmetric as well. Thus, $\hat{K}_\odot$ has some symmetry amongst its diagonal entries. We have to require

$$\hat{K}_\odot\Big|_{i+nj-n,i+nj-n} = \hat{K}_\odot\Big|_{j+ni-n,j+ni-n} \qquad \text{for all } i,j = 1,\dots,n.$$

Furthermore, the unit diagonal has to be preserved implying $\hat{K}_\odot\Big|_{i+ni-n,i+ni-n} = 1$ for all i. The operator $\hat{K}$ also has to preserve the positive definiteness. This restriction does not translate into a simple algebraic restriction on $\hat{K}_\odot$.

Before we can show that the matrix–matrix product ansatz also fits this structure, we need the definition of the Kronecker product of two matrices and a corollary, where the Kronecker product is the *tensor product* [26][2]:

Definition 1 The *Kronecker product* $C = A \otimes B \in \mathbb{R}^{no \times mp}$ of two matrices $A \in \mathbb{R}^{n \times m}$ and $B \in \mathbb{R}^{o \times p}$ is defined as

$$C = \begin{bmatrix} A_{11}B & A_{12}B & \cdots & A_{1m}B \\ A_{21}B & A_{22}B & \cdots & A_{2m}B \\ \vdots & \vdots & \ddots & \vdots \\ A_{n1}B & A_{n2}B & \cdots & A_{nm}B \end{bmatrix}.$$

Corollary 1 *For the Kronecker product and the vectorisation operator holds the following identity:*

$$vec(AXB) = (B^T \otimes A)vec(X),$$

where B^T is the transpose of B.

Proof The statement can be shown by computing each entry of the vector on the left-hand side and each entry of the vector resulting after the matrix vector product on the right hand side. Additionally, commutativity of real numbers is used. □

In the special case of $B = \mathbb{I}$, with $A = K_\ell$, $X = \mathcal{G}$, and $AX = \mathcal{G}^k$, we obtain

$$\begin{aligned} K_\ell \mathcal{G} = \mathcal{G}^k &\iff (\mathbb{I} \otimes A)\mathrm{vec}(\mathcal{G}) = \mathrm{vec}(\mathcal{G}^k) \\ &\iff \hat{K}_\ell \mathrm{vec}(\mathcal{G}) = \mathrm{vec}(\mathcal{G}^k). \end{aligned}$$

This means that we can represent the matrix-multiplication model (4) by requiring $\hat{K}_@$ to have the Kronecker product structure $\hat{K}_@ = (\mathbb{I} \otimes K)$. Again, the application $\hat{K}_@$ has to ensure that $\mathcal{G}^k$ is symmetric positive semi-definite and has a unit diagonal. We have

$$K_\ell \mathcal{G} = \mathcal{G}^k = (\mathcal{G}^k)^T = \mathcal{G}^T K_\ell^T = \mathcal{G} K_\ell^T.$$

Thus, K_ℓ has to be one solution of the Sylvester equation $X\mathcal{G} - \mathcal{G}X^T = 0$.

[2] According to some sources about history of mathematics, the definition tensor product should be attributed by G. Zehfuss, author of [26], even though Kronecker rediscovered it independently [8].

We could have equally well assumed that the K-operator corresponds to applying a matrix from the right, that is

$$\mathcal{G}^k = \mathcal{G}K_r. \tag{16}$$

In this case, we would have to impose the structure $\hat{K}_r = (K_r^T \otimes \mathbb{I})$. However, if we transpose (16), we obtain

$$(\mathcal{G}^k)^T = K_r^T \mathcal{G}^T \implies \mathcal{G}^k = K_r^T \mathcal{G},$$

since the correlation matrices are symmetric. Thus, $K_\ell = K_r^T$. That means that applying a matrix from the right does not lead to a different model as long as $\mathcal{G}$ and $\mathcal{G}^k$ are symmetric matrices.

Applying a single matrix from the left or the right is a difficult endeavour, since multiplying two matrices does generally not preserve symmetry. Thus, in particular, if we apply the same K_ℓ to the correlation matrices for multiple patients, then the resulting guess of $\mathcal{G}^k$ will generally not be symmetric.

It is, however, possible to apply matrices from the left and right simultaneously. That is, we could model $\mathcal{G}^k$ as

$$\mathcal{G}^k = K_\ell \mathcal{G} + \mathcal{G}K_r + K_1 \mathcal{G} K_2.$$

Using Corollary 1 three times yields

$$\hat{K}_{\text{mult}} = (\mathbb{I} \otimes K_\ell) + (K_r^T \otimes I) + (K_2^T \otimes K_1). \tag{17}$$

This is still a very structured form of $\hat{K}$. In this case, we have $4n^2$ parameters in (17) to define the n^4 entries of $\hat{K}$. To ensure symmetry preservation, it seems natural to assume $K_\ell = K_r^T$ and $K_1 = K_2^T$. Other choices might be able to preserve symmetry but are likely more cumbersome.

Of particular interest might be the special case where K_1 and K_2 are assumed to be 0. That is, we have

$$\hat{K}_{\text{mult}} = (\mathbb{I} \otimes K_\ell) + (K_r^T \otimes \mathbb{I}). \tag{18}$$

If we have multiple pairs of $(\mathcal{G}_i, \mathcal{G}_i^k)$, then we can write the model as

$$\begin{aligned} \mathcal{G}_1 K_r + K_\ell \mathcal{G}_1 &= \mathcal{G}_1^k \\ \mathcal{G}_2 K_r + K_\ell \mathcal{G}_2 &= \mathcal{G}_2^k \\ &\vdots \\ \mathcal{G}_q K_r + K_\ell \mathcal{G}_q &= \mathcal{G}_q^k. \end{aligned}$$

We now again use Corollary 1 but this time we vectorize K_r and K_ℓ instead of $\mathcal{G}_i$. This yields

$$\begin{bmatrix} \mathbb{I} \otimes \mathcal{G}_1 & \mathcal{G}_1^T \otimes \mathbb{I} \\ \mathbb{I} \otimes \mathcal{G}_2 & \mathcal{G}_2^T \otimes \mathbb{I} \\ \vdots & \vdots \\ \mathbb{I} \otimes \mathcal{G}_q & \mathcal{G}_q^T \otimes \mathbb{I} \end{bmatrix} \begin{bmatrix} \text{vec}(K_r) \\ \text{vec}(K_\ell) \end{bmatrix} = \begin{bmatrix} \text{vec}(\mathcal{G}_1^k) \\ \text{vec}(\mathcal{G}_2^k) \\ \vdots \\ \text{vec}(\mathcal{G}_q^k) \end{bmatrix}. \tag{19}$$

If q is equal to 2, this is a linear system of equations that most likely can be solved exactly. If $q > 2$, then this is an over-determined linear system and solving it should be understood in the linear least-squares sense.

This possibly over-determinant system of linear equations is large and only modestly sparse. The dimension is $qn^2 \times 2n^2$. Thus, for $n > 100$, the solution becomes quickly prohibitive.

Due to the symmetry, it is reasonable to require $K_r = K_\ell^T$. This could be added as a constraint in Eq. (19) or be used to reduce the number of unknowns. Alternatively, one can solve the unconstrained problem from Eq. (19) and then set K_ℓ to be the arithmetic mean of K_ℓ and K_r^T; and K_r the transpose of this mean.

There are two main problems with the approach in (19). The first problem is that for $q = 2$, we obtain a tailored K-operator for two patients. Experiments with pairs of healthy brains and brains affected by the disease from multiple patients show that the K-operator is over-fitted and really only works for the two patients used to compute K. If $q > 2$, then the least-squares error in (19) is relatively large. Furthermore, for the task of healing,

loosely associated with inverting K, restoring the original state is the best [15]. However, in some cases, achieving a state that can considered to be healthy may constitute a major step regarding the quality of life.

The second problem is that we can only infer the K-operator if we have correlation matrices of a healthy and a disease-affected state. This is often not the case, since, in many cases, diagnostic snapshots are only taken after the onset of symptoms, and we do not have data concerning the patient before symptoms of the disease were evident.

We address these problems in the next section.

5.1 Projection

We have seen in the previous section that preserving symmetry is causing some difficulties. These can be overcome by structural assumption on $\hat{K}$.

However, the previous section is mostly mute on enforcing positive definiteness in $\mathcal{G}^k$. Thus, we are now presenting an improved approach that ensures that after applying the K-operator, the result is a correlation matrix, a symmetric positive semi-definite matrix with unit diagonal.

We are particularly interested in the two subsets of correlation matrices that correspond to healthy and impaired brains. Let H be the subset of correlation matrices corresponding to healthy brains and I the subset corresponding to impaired brains. We do not know if H is a closed set or if H is convex. Contrary, since various different impacts can impair a brain, it seems unlikely that I is convex.

We now define $\tilde{K}$ as the composition of applying the operator $\hat{K}$ and a projection P that maps a matrix to the closest correlation matrix, that is, we use the model

$$\begin{aligned} &\tilde{K} \,:\, \mathbb{R}^{n\times n} \to \mathbb{R}^{n\times n} \,:\, \mathcal{G} \to \mathcal{G}^k \\ &\tilde{K} = P \circ \hat{K} \implies \tilde{K}(\mathcal{G}) = P(\hat{K}(\mathcal{G})). \end{aligned} \tag{20}$$

This ensures that the application of $\tilde{K}$ always leads to a correlation matrix. There are efficient ways to implement P iteratively on a computer; see, for instance, [9] or [4]. However, the authors are not aware of a closed form description of P. Equation 20 can also be considered as a special neural network with one standard layer recombining the inputs, that is the multiplication with $\hat{K}$, and one special layer that projects the result back to the set of correlation matrices, that is, the application of P. Thus, it is possible to use a stochastic gradient descent method to infer $\hat{K}$ from the data. Thereby $\hat{K}$ can be arbitrary or any of the special options discussed in the last section.

The automatic differentiation of P needed to efficiently compute a stochastic gradient descent is beyond the expertise of the authors and should be considered in the future. Thus, we consider this beyond the scope of our paper. In the next section, we discuss a toy example based on artificial data.

6 Discussion and conclusions

This section is devoted to demonstrating the previously described methods using a small artificial dataset. To this end, we use 5×5 correlation matrices. We consider the correlation matrix healthy if the correlation between two of the five random variables is between -0.3 and 0.3. Contrary, we consider a correlation matrix unhealthy if the correlation between at least two random variables exceeds 0.6 or is below -0.6. These numbers are simplifications of correlation matrices observed in the aforementioned open dataset on PD [12].

Participants with label PD-MCI show larger correlation partially above 0.6. The control group has mainly low, but non-negligible correlation, whilst participants with the label PD-NC have in some entries elevated correlations, often not reaching 0.6. The alteration of correlation often mirrors the change of network topology, with the increase of local connectivity in some areas, and the diminution of global connectivity, undermining the correct functioning of the overall brain.

The artificial data are generated using uniformly distributed random entries in the correlation matrix. We enforce symmetry by copying the lower triangular part onto the upper triangular part. We then align the signs in the unhealthy correlation matrix with the signs in the healthy correlation matrix. As a final step, we verify the desired properties. We reject the matrix and regenerate should the result fail to be positive definite. We also reject if our stipulations regarding the entries of healthy and unhealthy matrices are not fulfilled. Besides the diagonal, all entries of the healthy correlation matrix have to have an absolute value less or equal than 0.3. The unhealthy correlation matrix must have at least one off-diagonal entry exceeding an absolute value of 0.6.

Example 1 As a first experiment, we generate two pairs of healthy and unhealthy matrices, $(\mathcal{G}, \mathcal{G}^k)$ and $(\mathcal{G}_2, \mathcal{G}_2^k)$. We use the first pair to compute $K_\ell := \mathcal{G}^k\mathcal{G}^{-1}$, $K_r := \mathcal{G}^{-1}\mathcal{G}^k$ and $K_\odot = \mathcal{G}^k \odot \mathcal{G}^{\cdot -1}$.

We then compute the norms

$$\| \mathcal{G}^k - K_\ell \mathcal{G} \|, \quad \| \mathcal{G}^k - \mathcal{G} K_r \|, \quad \text{and} \quad \| \mathcal{G}^k - K_\odot \odot \mathcal{G} \| .$$

As expected all of these norms are close to machine precision. However, repeating the computation with the second pair shows large normwise deviations. This is also expected but underlines that all K-operators are over-fitted.

Example 2 In the second exam, we use the approach from (19). If we use $q = 2$ pairs as training data, that is, if we solve the equation exactly, then we observe that K_ℓ has a very large norm. This shows that the problem is very ill-conditioned. Applying K_ℓ and K_r to a test set of matrix pairs shows that the operator is extremely over-fitted and the normwise error

$$\| \mathcal{G}^k - (K_\ell \mathcal{G} + \mathcal{G} K_r) \|$$

is huge.

We also experimented with a larger training set of $q = 10$ and a test set of similar size. We obtain a normwise relative error

$$\| \mathcal{G}^k - (K_\ell \mathcal{G} + \mathcal{G} K_r) \| / \| \mathcal{G}^k \|,$$

of 0.35 on the training set and 0.49 on the test set. With a larger training set, the error on the test set can be reduced. For instance, $q = 100$ leads to an error of 0.40 on a test set of 100 pairs.

With the current setup, the result indicates that this more general K-operator is still over-fitted. It also shows that the generalised K-operator can only capture between $\frac{1}{2}$ and $\frac{2}{3}$ of the changes.

These examples concern global prediction quality. However, rather than a use as a general classifier, a key usefulness of the K-operator is the focus on specific submatrices where the changes are more relevant. Thus, the operator can be used as a "filter" to focus the attention on specific entries, extending later the analysis with other techniques, as it has been done in [6], with the comparison of recurrence plots of two regions highlighted by it. Thus, the operator can constitute a probe towards further and more detailed analyses, as a lens to look through high-dimensional data, as a tool to select features.

That said, being motivated by the medical relevance of the information obtained through K in preliminary data-based studies [13,16], and warned by the overfitting estimations presented in the examples above, future analysis involving a higher number of patients from different datasets can assess the disease-weighted impact of those changes identified by the operator, and help refine its definition itself.

Understanding the limitations of a new approach is a step towards its refinement. The problem of a general yet not-overfitting definition of the K-operator is still open, and it constitutes a fascinating challenge between mathematics, physics, and neurology.

Acknowledgements The authors thank Alessandro Pensabene, of the University of Palermo, for the information concerning the PD dataset.

Funding Information Open access funding provided by Consiglio Nazionale Delle Ricerche (CNR) within the CRUI-CARE Agreement. The research by M. M. is supported by the Project funded by Next Generation EU—"Age-It—Ageing well in an ageing society" (PE0000015), National Recovery and Resilience Plan (NRRP)—PE8—Mission 4, C2, Intervention 1.3.
The research by T. M. has been partially funded by the Deutsche Forschungsgemeinschaft (DFG)—Project-ID 318763901—SFB1294.

Data Availability Statement Data of the considered patients can be accessed at https://openneuro.org/datasets/ds005892/versions/1.0.0 [12].

Declarations

Conflict of interest The authors declare no conflict of interest.

Ethics approval and consent to participate Not applicable from the side of the authors of this article. Data were already collected by the authors of [12], during a study approved by the Institutional Review Board (IRB) at New York University (NYU), for which all participants provided informed consent.

Code availability The code for the presented examples can be accessed via GitHub (https://github.com/medusamedusa/K-operator_comparative_tests) and CodeBerg (https://codeberg.org/medusamedusa/K-operator_comparative_tests).

References

1. S. Achard, E. Bullmore, Efficiency and cost of economical brain functional networks. PLoS Comput. Biol. **3**(2), e17 (2007)
2. M. Banwinkler, H. Theis, S. Prange, T. van Eimeren, Imaging the Limbic System in Parkinson's Disease–A Review of Limbic Pathology and Clinical Symptoms. Brain Sci. **12**(9), 1248 (2022)
3. F. Blandini, G. Nappi, C. Tassorelli, E. Martignoni, Functional changes of the basal ganglia circuitry in Parkinson's disease. Prog. Neurobiol. **62**(1), 63–88 (2000)
4. R. Borsdorf, N.J. Higham, A preconditioned newton algorithm for the nearest correlation matrix. IMA J. Numer. Anal. **30**(1), 94–107 (2010)
5. H. Cui, et al, Interpretable Graph Neural Networks for Connectome-Based Brain Disorder Analysis. In L. Wang, Q. Dou, P. T. Fletcher, S. Speidel, and S. Li, editors, Medical Image Computing and Computer Assisted Intervention – MICCAI 2022, volume 13438 of Lecture Notes in Computer Science, Cham, (2022). Springer
6. S. Fazio, P. Ribino, F. Gasparini, N. Marwan, P. Fazio, M. Gherardi, M. Mannone, *K*-operator for Modelling Neurodegeneration: Simulations, fMRI Application, Eigenvalue Analysis and Recurrence Plots. Journal of Medical Systems, (2025), accepted for publication
7. V. Filyushkina, V. Popov, R. Medvednik, V. Ushakov, A. Batalov, A. Tomskiy, I. Pronin, A. Sedov, Hyperactivity of Basal Ganglia in Patients With Parkinson's Disease During Internally Guided Voluntary Movements. Front. Neurol. **7**(10), 847 (2019)
8. H.V. Henderson, F. Pukelsheim, S.R. Searle, On the history of the kronecker product. Linear and Multilinear Algebra **14**(2), 113–120 (1983)
9. N.J. Higham, Computing the nearest correlation matrix-a problem from finance. IMA J. Numer. Anal. **22**(3), 329–343 (2002)
10. Q.J.M. Huys, T.V. Maia, M.J. Frank, Computational psychiatry as a bridge from neuroscience to clinical applications. Nat. Neurosci. **19**(3), 404–413 (2016)
11. X. Jia et al., Progressive Prefrontal Cortex Dysfunction in Parkinson's Disease With Probable REM Sleep Behavior Disorder: A 3-Year Longitudinal Study. Front Aging Neurosci. **10**(13), 750767 (2022)
12. A.S. Kemp, J. Eubank, Y. Younus, J.E. Galvin, F.W. Prior, Larson-Prior L. J. Resting State MRI data from healt hy control (HC), Parkinson's disease with normal cognition (PD-NC), and Parkinson's disease with mild cognitive impairment (PD-MCI) cohorts. OpenNeuro. [Dataset], (2025)
13. M. Mannone, P. Fazio, J. Kurths, P. Ribino, N. Marwan, *A Brain Network Operator for Modeling Disease: A First Data-Based Application for Parkinson's Disease* (European Physical Journal, Special Topics, 2024)
14. M. Mannone, P. Fazio, N. Marwan, Modeling a Neurological Disorder as the Result of an Operator Acting on The Brain: A First Sketch Based on Network Channel Modeling. Chaos, 34(5), (2024)
15. M. Mannone, P. Fazio, P. Ribino, N. Marwan, On disease and healing: a theoretical sketch. Frontiers in Applied Mathematics and Statistics, 10, (2024)
16. M. Mannone, N. Marwan, P. Fazio, P. Ribino, Limbic and cerebellar effects in Alzheimer-Perusini's disease: A physics-inspired approach. Biomed. Signal Process. Control **103**, 107355 (2025)
17. M. Mannone, P. Ribino, P. Fazio, N. Marwan, Sketching a Space of Brain States. Neuroinformatics, (2025)
18. M. Mannone, P. Ribino, A. Saibene, P. Fazio, S. Fazio, F. Gasparini, M. Gherardi, N. Marwan, Computing the Time-dependent Krankheit-operator in Epilepsy from ECoG: a Case Study. In S. Y. Yurish, editor, Proceedings of the 7th International Conference on Advances in Signal Processing and Artificial Intelligence (ASPAI' 25), Innsbruck, Austria, (2025). IFSA
19. P.E. Mosley, G.A. Robinson, Functional network reorganization precedes apathy in Parkinson's disease: a neural marker of risk? Brain **146**(7), 2661–2662 (2023)
20. I.M. O'Shea, H.S. Popal, I.R. Olson, *et al.*, Distinct alterations in cerebellar connectivity with substantia nigra and ventral tegmental area in Parkinson's disease. Sci Rep, 12(3289), (2022)
21. O. Sporns, G. Tononi, R. Kötter, The human connectome: A structural description of the human brain. PLoS Comput. Biol. **1**(4), e42 (2005)
22. M. Tops, Are the insular cortex and cortisol implicated in Parkinsonian features? Parkinsonism & Related Disorders **12**(8), 467–471 (2006)
23. G. Varoquaux, A. Gramfort, F. Pedregosa, V. Michel, B. Thirion, Multisubject dictionary learning to segment an atlas of brain spontaneous activity, in *Information Processing in Medical Imaging (IPMI 2011)*. ed. by G. Székely, H.K. Hahn. pp. (Springer, Cham, 2011), pp.562–573

24. B.A. Vogt, Cingulate cortex in Parkinson's disease. Handb. Clin. Neurol. **166**, 253–266 (2019)
25. M. Yuan, D. Na, Z. Song, Primary motor area-related injury of anterior central gyrus in Parkinson's disease with dyskinesia: A study based on MRS and Q-space. Neurosci. Lett. **805**, 137224 (2023)
26. G. Zehfuss, Ueber eine gewisse Determinante. Zeitschrift für Mathematik und Physik **3**, 298–301 (1858)
27. Z.W. Zhan, L.Z. Lin, E.H. Yu, J.W. Xin, L. Lin, H.L. Lin, Q.Y. Ye, X.C. Chen, X.D. Pan, Abnormal resting-state functional connectivity in posterior cingulate cortex of Parkinson's disease with mild cognitive impairment and dementia. CNS Neurosci. Ther. **24**(10), 897–905 (2018)